Supporting Information

Controllable Unzipping of Carbon Nanotubes as Advanced Pt Catalyst Supports for Oxygen Reduction

Qingzhu Shu[ab], Zhangxun Xia[b], Wei Wei[b], Xinlong Xu[b], Ruili Sun[b], Ruoyi Deng[b], Quanhong Yang[c] , Hong Zhao*[a], Suli Wang*[b], Gongquan Sun*[b]

a. The College of Materials Science and Engineering, Dalian Jiao tong University, 794 Huang he Road, Dalian Liaoning, 116028, China. E-mail: zhaohong@djtu.edu.cn

b. Division of Fuel Cell & Battery, Dalian National Laboratory for Clean Energy, Dalian Institute of Chemical Physics, Chinese Academy of sciences, Dalian, China 116023, E-mail: suliwang@dicp.ac.cn; gqsun@dicp.ac.cn

c. Nanoyang Group, School of Chemical Engineering and Technology, Collaborative Innovation Center of Chemical Science and Engineering (Tianjin), Tianjin University, Tianjin, 300072, China.

1. Additional analysis of unzipped MWCNT

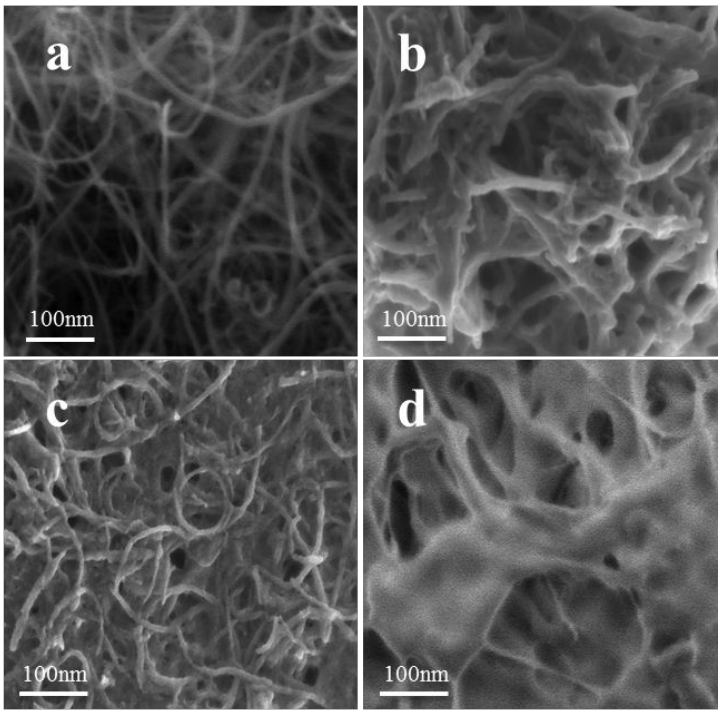

Figure S1. (a~d) SEM images of MWCNT, LU-MWCNT, MU-MWCNT and HU-MWCNT, respectively, which intuitive expression of the structural changes of MWCNTs with the opening strength increased.

.

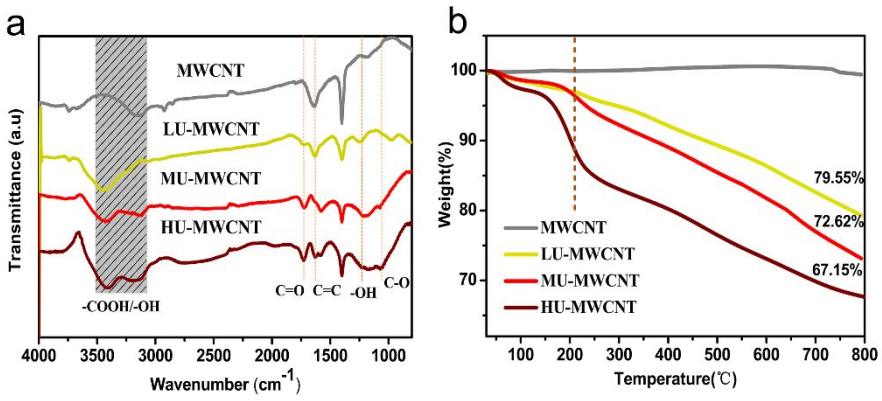

Figure S2. (a) FTIR spectra of the different carbon materials; mainly exhibits the characteristic peaks of hydrophilic oxygenated groups; (b) TGA weight loss curves of the four samples; as the level of oxidation increases, the total amount of weight loss is increased.

2. Additional analysis of Pt/unzipped-MWCNT catalysts

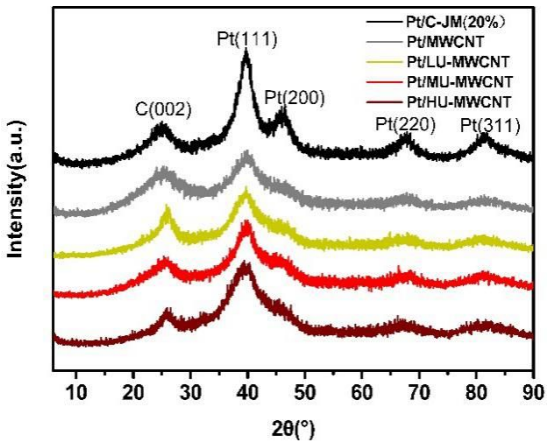

Figure S3. XRD patterns of commercial Pt/C, Pt/LU-MWCNT, Pt/MU-MWCNT and Pt/HM-MWCNT. The Pt loading was ca. 20 wt%.

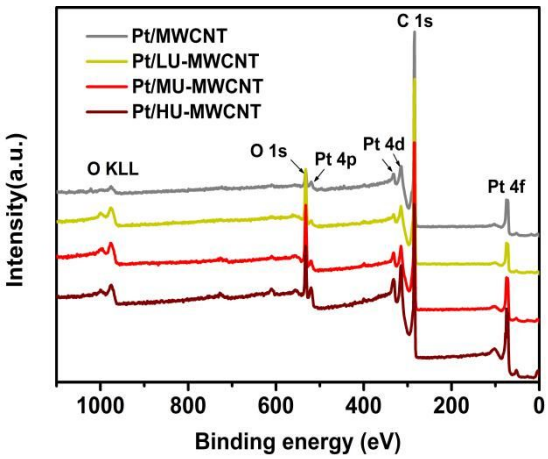

Figure S4. The XPS survey spectrum and high-resolution of Pt/MWCNT, Pt/LU-MWCNT, Pt/MU-MWCNT and Pt/HU-MWCNT.

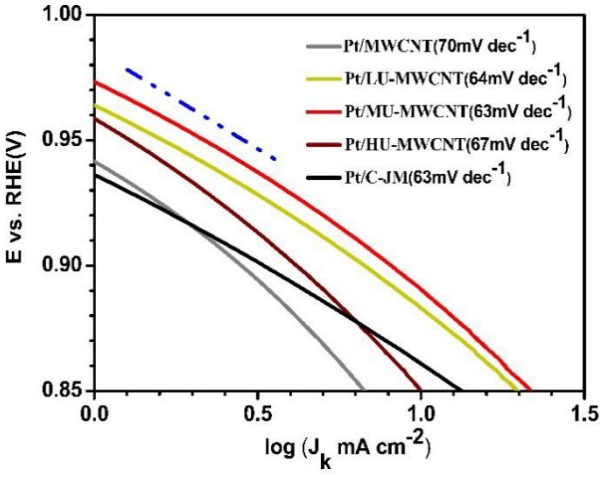

Figure S5. Tafel plots of Pt/unzipped-MWCNT and Pt/C-JM: according to the ORR polarization curve, the dynamic current densities of different samples were calculated, and their logarithms were taken as abscissa and potentials as ordinate.

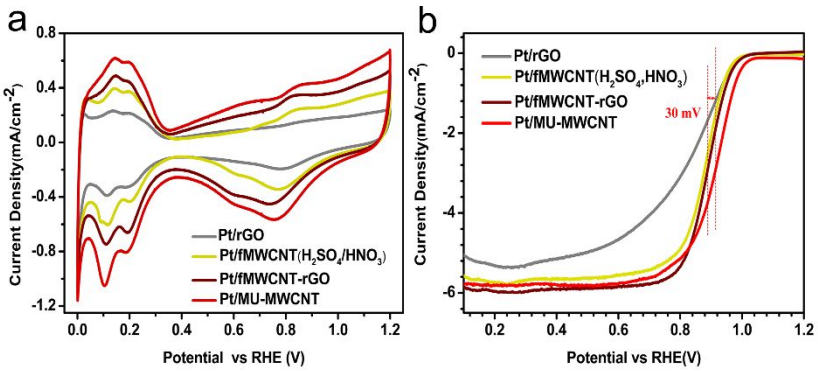

Figure S6. (a) The CV comparison diagram of Pt/rGO, Pt/fMWCNT, Pt/fMWCNT-rGO and Pt/MU-MWCNT catalysts with a scan rate of 10 mV s^{-1} in N_2 saturated 0.1M $HClO_4$; (b) LSV results for different samples in O_2 saturated atmosphere.

GO was first synthesized from graphite by a modified Hummer's method and then loaded with Pt nanoparticles in the same way as before, the Pt/rGO catalyst was obtained after reduction at low temperature in hydrogen environment. The preparation of functional MWCNT (fMWCNT) refers to the method in literature “Nano Research 2016, 9(2): 329–343”: A pristine MWCNT (5.0 g), HNO_3 (65%, 100 mL, 1.465 mol) and H_2SO_4 (98%, 300 mL, 5.52 mol) were added into a 1,000 mL flask equipped with a condenser under vigorous stirring. The flask was immersed in an ultrasonic bath for 30 min, and then stirred for 30 min under reflux at 80 C. This process was repeated 6 times. After cooling to room temperature, the reaction mixture was diluted with 500 mL of deionized (DI) water and then vacuum-filtered through filter paper (Fisher). The dispersion, filtering, and washing steps were repeated until the pH of the filtrate reached to about 7. The filtered solid was dried under vacuum for 24 h at 60 C, affording fMWCNT. Then, GO and fMWCNT were mixed in a mass ratio of 1:1, a certain amount of deionized water was added. The mixture was stirred for 24 hours to make it physically interwoven to form a three-dimensional structure. After loading of Pt nanoparticles, the solid was also reduced at low temperature in hydrogen atmosphere to prepared Pt/rGO-fMWCNT. The oxygen reduction performance of Pt/MU-MWCNT was compared with that of Pt/rGO, Pt/fMWCNT and Pt/rGO-fMWCNT which was in order to highlight the unique three-dimensional structure and better catalytic

performance of MU-MWCNT compared with carbon materials treated by traditional methods.

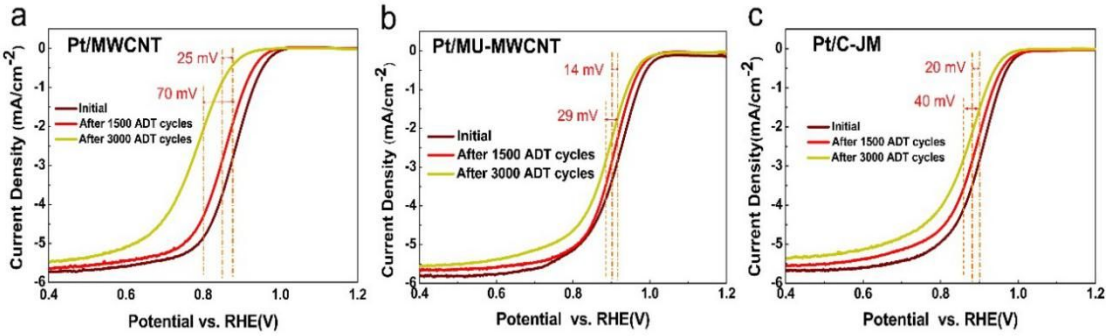

Figure S7. ORR polarization curves of (a) Pt/MWCNT, (b) Pt/MU-MWCNT and (c) Pt/C-JM before and after ADT tests.

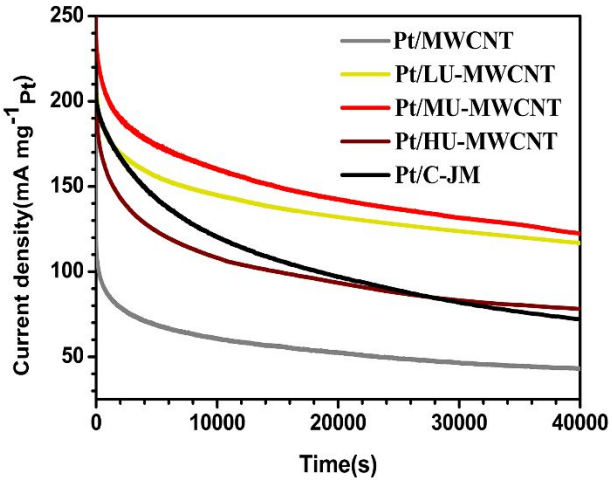

Figure S8. Chronoamperometry (CA) measurements of the different catalysts in O_2 saturated 0.1 M $HClO_4$ solution on the constant potential of 0.6 V(vs. RHE) for 40000 s at a rotation rate of 1600 rpm under room temperature.

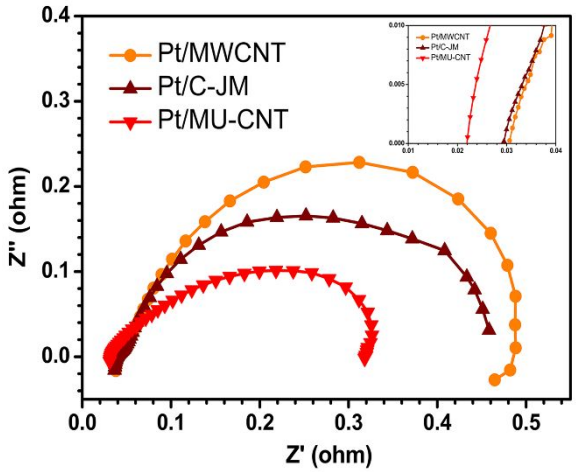

Figure S9. Electrochemical impedance spectra of DMFC with different cathode catalysts of Pt/MWCNT, Pt/C-JM and Pt/MU-CNT at constant current density of 100 mA cm^{-2}.

Table S1 Performance comparison of oxygen reduction catalysts based on different carrier materials reported in literatures

Catalyst	BET surface area (m^2 g^{-1}) of the carbon support	Mean particle size (nm)	ECSA (m^2 g_{Pt}^{-1})	$E_{1/2}$	Tafel (mV/dec)	Mass Activity , MA (A/mg_{Pt})	Cell performance	Refrence
Pt/XC-72	254	2.6	99.79	-	86.6	0.065(0.9V)	No battery test characterization	[1]
Pt/BP2000	1450	3.3	54.0	-	71.1	0,0687(0.7V)	No battery test characterization	[2]
Pt/rGO	3.2	4.56±0.08	14.0	0.87(vs. RHE)	84	0.092(0.9V)	maximum power density was 56.3 mW mg_{Pt}^{-1} cm^{-2}: 80℃, H_2, 0.12 cm^3 min^{-1} and O_2: 0.10 cm^3 min^{-1}.	[3]
Pt/MWCNT	51	2.6	-	-	-	0.0147(0.8V)	maximum power density was 103	[4]

							mW/cm^2; 90℃; 1 M CH_3OH: 1 mL/min; O_2: 0.2 MPa	
Pt/GNP_{500}	1000	4.4	26.69	0.8(vs. NHE)	60	0.0801(0.8V)	No battery test characterization	[5]
Pt/CNT-MWH	60	2.7	70	-	-	0,060(0.9 V)	peak power density was 365 mWcm^{-2}: 55 ℃, pure H_2 and O_2 gases were passed at anode and cathode side, respectively	[6]
Pt/TiO_2-MWCNT	-	-	-	0.83±0.01(vs. RHE)	61±6	0.067±0.002(0.9 V)	No battery test characterization	[7]
Pt/RGO-CB	-	5	56.4	0.83(vs. RHE)	-	0.158(0.9 V)	No battery test characterization	[8]
PtCo/Co@NHPCC	356		64.6	0.883(vs.RHE)	59	0.566(0.9V)	No battery test characterization	[9]
Pt–WN/CNT-rGO	281.1	3	85.21	0.85(vs. RHE)	55	151.3(0.9)	No battery test characterization	[10]
MWCNT-Pt (2 : 1)	-	2 - 4	43.6	-	-	-	peak power density was 28.5 ± 0.2 mW cm^{-2}; 25±1℃; 2 M methanol; Air	[11]
Pt/CB	222	4.5	-	0.862 (vs.RHE)	-	-	peak power density was 95 mW cm^{-2}; 60℃; 1 M methanol solution: 3 mL/min; Air: 400 mL/min.	[12]

Pt/MU-MWCNT	338.2	2	103.4	0.915(vs.RHE)	63	174.5	peak power density was 106 mW cm^{-2}.; 80℃; 0.5 M methanol solution: 1 mL/min; Air: 100 mL/min.	This work

References

(1) Teran-Salgado, E.; Bahena-Uribe, D.; Márquez-Aguilar, P. A.; Reyes-Rodriguez, J. L.; Cruz-Silva, R.; Solorza-Feria, O. Platinum nanoparticles supported on electrochemically oxidized and exfoliated graphite for the oxygen reduction reaction. *Electrochim. Acta* 2019, 298, 172-185.

(2) Ying, J.; Li, J.; Jiang, G.; Cano, Z. P.; Ma, Z.; Zhong, C.; Su, D.; Chen, Z. Metal-organic frameworks derived platinum-cobalt bimetallic nanoparticles in nitrogen-doped hollow porous carbon capsules as a highly active and durable catalyst for oxygen reduction reaction. *Appl. Catal., B* 2018, 225, 496-503.

(3) Sakthivel, M.; Drillet, J.-F. An extensive study about influence of the carbon support morphology on Pt activity and stability for oxygen reduction reaction. *Appl. Catal., B* 2018, 231, 62-72.

(4) Hussain, S.; Erikson, H.; Kongi, N.; Tarre, A.; Ritslaid, P.; Rähn, M.; Matisen, L.; Merisalu, M.; Sammelselg, V.; Tammeveski, K. Pt nanoparticles sputter-deposited on TiO2/MWCNT composites prepared by atomic layer deposition: Improved electrocatalytic activity towards the oxygen reduction reaction and durability in acid media. *Int. J. Hydrogen Energy* 2018, 43, 4967-4977.

(5) Pu, L.; Zou, L.; Zhou, Y.; Zou, Z.; Yang, H. High performance MWCNT–Pt nanocomposite-based cathode for passive direct methanol fuel cells. *RSC Adv.* 2017, 7, 12329-12335.

(6) Bharti, A.; Cheruvally, G.; Muliankeezhu, S. Microwave assisted, facile synthesis of Pt/CNT catalyst for proton exchange membrane fuel cell application. *Int. J. Hydrogen Energy* 2017, 42, 11622-11631.

(7) Yan, H.; Meng, M.; Wang, L.; Wu, A.; Tian, C.; Zhao, L.; Fu, H. Small-sized tungsten nitride anchoring into a 3D CNT-rGO framework as a superior bifunctional catalyst for the methanol oxidation and oxygen reduction reactions. *Nano Res.* 2016, 9, 329-343.

(8) Kim, J.; Jang, J.-S.; Peck, D.-H.; Lee, B.; Yoon, S.-H.; Jung, D.-H. Methanol-tolerant platinum-palladium catalyst supported on nitrogen-doped carbon nanofiber for high concentration direct methanol fuel cells. *Nanomater.* 2016, 6, 148.

(9) Li, Y.; Li, Y.; Zhu, E.; McLouth, T.; Chiu, C.-Y.; Huang, X.; Huang, Y. Stabilization of high-performance oxygen reduction reaction Pt electrocatalyst supported on reduced graphene oxide/carbon black composite. *J.*

Am. Chem. Soc. 2012, 134, 12326-12329.

(10) Xu, F.; Wang, M.-x.; Liu, Q.; Sun, H.-f.; Simonson, S.; Ogbeifun, N.; Stach, E. A.; Xie, J. Investigation of the carbon corrosion process for polymer electrolyte fuel cells using a rotating disk electrode technique. *J. Electrochem. Soc.* 2010, 157, B1138-B1145.

(11) Wang, M.; Xu, F.; Liu, Q.; Sun, H.; Cheng, R.; He, H.; Stach, E.; Xie, J. Enhancing the catalytic performance of Pt/C catalysts using steam-etched carbon blacks as a catalyst support. *ECS Trans*. 2010, 33, 507-531.

(12) Li, W.; Liang, C.; Zhou, W.; Qiu, J.; Zhou, Z.; Sun, G.; Xin, Q. Preparation and characterization of multiwalled carbon nanotube-supported platinum for cathode catalysts of direct methanol fuel cells. *J. Phys. Chem. B* 2003, 107, 6292-6299.